Estimating the Dimensions of Weather and Climate Attractors

KLAUS FRAEDRICH

Institut für Meteorologie, Freie Universität Berlin, D-1000 Berlin 41

(Manuscript received 4 June 1985, in final form 16 September 1985)

ABSTRACT

The dimensions of attractors are estimated from phase space trajectories of observed weather and climate variables (local surface pressure and relative sunshine duration, zonal wave amplitude; a δ^{18}O-record). They provide primary information for descriptions of properties of the attractors of dynamical systems and give a lower limit to the number of the essential variables necessary to model the dynamics. These estimates are based on distance distributions of pairs of points on the single variable trajectory evolving in phase spaces which embed the attractor. One observes a low fractal dimensionality between three and four for the weather attractor, if interannual variability and seasonal changes are eliminated. The physical interpretation is based on the three dominating scales of cyclones, cyclone families and index-cycle; the irregularity of the flow and strong dependence on initial conditions account for the fractal value. The climate variable also reveals a low dimensionality (between four and five) of the climate attractor. This is supported by an independent estimate based on eigenfunction expansion of the embedded phase space trajectory. These types of analyses suggest how to extend the standard data evaluation and model verification techniques to an analysis of the phase space behavior of observed and simulated dynamical systems.

1. Introduction

Standard atmospheric circulation statistics provide physical information in terms of means, covariances and, occasionally, space–time filtered or cross-spectral properties of the basic meteorological field variables: mean temperatures, eddy heat fluxes, energy conversions in appropriate space-time or wavenumber-frequency domains. In this sense physical bulk properties of the underlying dynamics define weather or climate. Another type of data analysis is the phenomenological circulation statistic. It is closely related to the real weather phenomena: storm tracks of tropical and extratropical cyclones, regional cyclone frequency depending on their life cycle and the prevailing season, etc. These statistics account for the individual weather patterns and lead to the phenomenological aspects of the dynamical system. Both types of statistics describe two aspects of the same physical processes and contribute different information to it. In this study we describe and apply a further method of analysis to evaluate the dynamics of the weather or climate system. It complements the other two statistical approaches or data analyses in the sense that mathematical properties are deduced.

Flows observed in the atmosphere and other hydrodynamic systems reveal a hierarchy of structures that range from laminar to turbulent motions. Despite the complexity of these flows there are many attempts to describe the behavior by nonlinear models depending on a few variables only (e.g., Charney and DeVore, 1979). These modeling efforts seem to be guided by the hypothesis that the basic structures of the observed flows depend on a finite and possibly small number of parameters that control it, i.e., a few degrees of freedom or a low dimensionality of the system as it evolves in phase space. On the other hand, there are recent analyses of hydrodynamic experiments made to obtain such dimensionality estimates from observations; there is evidence that a relatively small number of degrees of freedom characterizes observed turbulent flows. Guckenheimer and Buzyna (1983) analyze the transition to geostrophic turbulence in a rotating annulus and reveal a low dimensionality for the vacillation regime turning into a turbulent one. Brandstäter et al. (1983) present empirical evidence for turbulent flows (which evolve in a low dimensional subspace of the whole phase space) when analyzing modulated wavy vortices (Couette–Taylor flow). Finally, Nicolis and Nicolis (1984) used the isotope record of a deep sea core with relatively few data points, to estimate the degrees of freedom which govern the observed long-term climate evolution during the past million years; they also obtained a low dimensionality (between three and four) for the climate system. The analyses of observations are based on statistical procedures which lead to measures of dimensionality or degrees of freedom which control the underlying dynamics (e.g., Grassberger and Procaccia, 1983a,b). But these methods of data analysis also provide an objective test for the quality of model solutions because they give a quantitative measure for its time evolution (in phase space).

In this study various time series are analyzed to estimate the minimum number of independent variables

(degrees of freedom) necessary to model the time evolution and the number of variables sufficient to do so. The analysis is based on similar procedures; its methodological background is described in section 2, applications are presented in section 3. Furthermore, an independent estimate of dimensionality is introduced (section 4) and applied to a climate record.

2. Basic concepts

The dynamics of the weather and climate system is simulated by partial differential equations describing the underlying physical processes. These equations can be transformed to a set of n time dependent ordinary differential equations, if the space variability is expanded into a set of n orthogonal functions. A typical example is the spectral truncation of the hydrodynamic equations for the atmospheric flow (e.g., Silberman, 1954). The resulting set of ordinary differential equations defines the time development of n expansion coefficients $x_j(t)$:

$$\dot{x}_j = f_j(x_1, \cdots x_n); \quad j = 1, \cdots, n.$$

Thus the phase space containing the time evolution of the underlying process is spanned by the n different variables x_j, $j = 1, \cdots, n$ of the dynamical system. Portraits of the time evolution of the system are formed by trajectories in this n-dimensional phase space. They exhibit distinct patterns, called attractors which trap trajectories after transients originating from the initial states decreased. All initial values, whose trajectories are captured by the attractor, define the attractor basin. In characterizing these attractors one may follow the common "roads to turbulence in dissipative dynamical systems" (Eckmann, 1981). There are one or more steady states (i.e., zero-dimensional points) which belong to related attractor basins; periodic orbits or limit cycles are one-dimensional closed lines and quasi-periodicity occurs on two-dimensional tori in phase space. Irregular or chaotic motions can appear on strange attractors in three and higher dimensional phase spaces. A first example related to atmospheric processes has been presented by Lorenz (1963). Although deterministic, the dynamics of these systems reveal chaotic or irregular behavior, which is realized by a sensitive dependence on initial conditions—a feature of the weather and climate system.

The attracting sets (or attractors) form invariant manifolds of the dynamical systems, which often have dimensions d smaller than those of the phase space $d < n$. Here it should be noted that attractors with irregular behavior are not necessarily confined to integer dimensions; fractals or noninteger dimensions (Mandelbrot, 1977) seem to be common for many turbulent systems which are deterministic with a strong sensitivity on initial conditions and show features, which appear—to a certain degree—irregular or chaotic.

The attractor of a dynamical system is represented by the asymptotic limits of trajectories in a phase space spanned by those independent variables, which define the dynamics. If information and topological (geometrical) properties (such as the dimension) of attractors are to be evaluated from observations, one is generally confined to time series of a single state variable sampled at regular time intervals Δt. To deduce such measures from observed turbulent or chaotic flows, Packard et al. (1980) suggest a reconstruction of the phase space picture of the attractor. This can be achieved by transforming the dynamic process into a new phase space of successively higher dimension until no more information is gained by adding a further independent coordinate. The single variable time series (or observable) represents one such coordinate; its $(m - 1)$ derivatives or, in the discrete case, the $(m - 1)$ lagged time series shifted by $(m - 1)$ multiples of the correlation time τ provide further independent coordinates (subsection 2a). Phase portraits of the time evolution of the dynamical system can now be constructed in this new m-dimensional phase space spanned by the single state variable and its successive derivatives (or time shifted variables).

a. Embedding

The set of n ordinary differential equations

$$\dot{x}_j = f_j(x_1, \cdots, x_n); \quad j = 1, \cdots, n \qquad (2.1)$$

describes the dynamics of weather and climate in an n-dimensional phase space. The phase space is spanned by n coordinates $x_j, j = 1, \cdots, n$ which are defined by the n independent variables of the dynamical system. Thus the time evolution is given by a vector $\xi(t)$:

$$\xi(t) = [x_1(t), \cdots, x_n(t)], \qquad (2.2)$$

whose components define the position of the trajectory in the phase space. The system (2.1) can be reduced to a single highly nonlinear differential equation for one of the variables $x_j(t)$, say $x(t)$, if all others are eliminated by differentiation. This leads to an nth order differential equation

$$x^{(n)} = f[x, x', \cdots, x^{(n-1)}], \qquad (2.3)$$

which is equivalent to a set of n equations describing the time evolution, $x(t)$, plus its $n - 1$ derivatives $x(t)$, $x'(t), \ldots, x^{(n-1)}(t)$:

$$\mathbf{x}(t) = [x(t), x'(t), \cdots, x^{(n-1)}(t)]. \qquad (2.4a)$$

The initial value problem (i.e., Cauchy boundary conditions) posed by the single state variable $x(t)$ and its $n - 1$ successive derivatives starts the time evolution (2.3) or (2.4a) which appears in the same n-dimensional phase space of n coordinates [i.e., the time series plus its $(n - 1)$ derivatives]. This is represented by the vector components (2.4a) which define the position of the trajectory of the time evolution. Adding further derivatives

[e.g., $x^{(n)}(t)$] to the vector (2.4a) is superfluous, because it does not produce more independent information.

Now, if a manifold within the original n-dimensional phase space $x_1, \ldots, x_n$ (2.1), (2.2) is considered (say, an attractor or any other geometrical object of dimension $d \ll n$) it can be described in the new phase space $x, x', x'', \ldots$ spanned by the single variable and its derivatives (2.3), (2.4). It should be noted that the dimensionality of the new phase space may be smaller than that of the original phase space. This is an embedding which is based on a sound mathematical background; the Whitney embedding theorem (Takens, 1981; Whitney, 1936; Hirsch, 1976) which is valid for almost all smooth dynamical systems. The theorem implies that d-dimensional manifolds (described by the dynamical system (2.1) and evolving in the n-dimensional phase space with coordinates $x_j, j = 1, \cdots, n$) can be embedded into an $(m = 2d + 1)$-dimensional space (e.g., spanned by the variable $x(t)$ and its second successive derivatives which define the embedded dynamics). The theorem, which requires an embedding dimension $m = 2d + 1$, places the analysis (of dimensionality of attractors by embedding) on the safe side; to evaluate dimensions of attractors of physical systems it suffices to guarantee embedding dimensions m sufficiently larger than those of the attractors, which are generally of lesser dimensionality than that of the original phase spaces ($d < m, n$). Here it should be noted that the theorem of Takens (1981) has not yet been proved in such generality that it includes general attractors with fractal dimensionality (because these are no manifolds). But it seems plausible that a general version of the theorem of Takens may be formulated, however, requiring an embedding dimension in growing with d^2 rather than $2d + 1$ (personal communication, 1985).

Thus, for deriving the dimension of attractors from single state variables it is sufficient to embed them into an m-dimensional space spanned by the time series and its $m - 1$ derivatives:

$$\mathbf{x}(t) = [x(t), \cdots, x^{(m-1)}(t)], \tag{2.4b}$$

i.e., it is not necessary to know the original phase space (or independent state variables) and its dimension n as long as m is chosen large enough. Instead of the continuous variable $x(t)$ and its derivatives, $x^{(m-1)}(t)$, a discrete time series $x(t)$ and its shifts by $(m - 1)$ time lags $(m - 1)\tau$ may be considered to identify structures in the time evolution of the single state variable (Ruelle, 1981)

$$\mathbf{x}(t) = \{x(t), x(t + \tau), \cdots, x[t + (m - 1)\tau]\}. \tag{2.4c}$$

This is particularly useful, if the dynamical variables are observables which, in most cases, are discrete. Here it should be noted that in analogy with the continuous case the time shifted coordinates should be linearly independent (i.e., differentiation is a linear operator). For observables this can be achieved by choosing the macrotime scale (or autocorrelation time) τ as a lower limit of the basic time step. This is plausible because vanishing autocorrelations guarantee uncorrelated (statistically independent) data; they are also linearly independent (whereas the reverse does not hold) because a vanishing dot-product (i.e., the autocorrelation) defines orthogonality.

If attractors of observed or simulated dynamical systems and their topological properties are investigated, it is sufficient to consider a single state variable, $x(t)$, and its time trajectory in a phase space spanned by the time shifted coordinates (2.4). In the following sections we are concerned with estimates of the dimensions of weather and climate attractors using only a single observable and embedding it in a phase space of time shifted coordinates. The methods of deducing the dimension are discussed in the following subsections. The estimates are based on general considerations of the dimensionality (Grassberger and Procaccia, 1983a,b; Ben-Mizrachi et al., 1984) and empirical orthogonal functions.

b. Dimension

An intuitive approach toward a general definition of dimension may be gained, if one considers a simple geometrical object. A cube of the dimension d and the volume V is filled by a number $N(L)$ of smaller boxes with the sidelength L. Then the total volume yields

$$V = \sum_{N(L)} L^d = N(L)L^d, \tag{2.5}$$

i.e., the number of boxes, $N(L)$, needed to fill the volume grows with decreasing sidelength according to $N(L) = VL^{-d}$; the dimension d can now be eliminated from $L^d = V/N(L)$:

$$d = \ln N(L)/(\ln L_0/L) + (\ln V/V_0)/(\ln L/L_0), \tag{2.6}$$

where unit scales V_0, L_0 are introduced for convenience. Taking the limit of decreasing sidelength of the boxes, $L \to 0$, the last term vanishes. This leads to the more general definition of dimension (or capacity):

$$d = \lim_{L \to 0} [\ln N(l)/(\ln L_0/L)]. \tag{2.7}$$

It is called a Hausdorff or fractal dimension (e.g. Mandelbrot, 1977), because it allows noninteger values to characterize geometrical objects (e.g., strange attractors in phase space). Thus the definition of dimension is generalized, if one considers a volume of dimension d filled by a number of volume elements of the sidelength L; this number $N(L)$ grows exponentially (d) with decreasing sidelength. One may now reformulate (2.7):

$$N(L) = (L/L_0)^{-d} \quad \text{for} \quad L \to 0. \tag{2.8}$$

The exponent d (Hausdorff dimension or capacity) determines a growth rate, which describes how the number of boxes $N(L)$ needed to cover the attractor

set increases with decreasing sidelength L. This result may be used to determine the dimension d by plotting $\ln N$ against $\ln L_0/L$. Such a box counting algorithm, however, appears to be impractical for calculating the dimensionality of strange attractors, because it converges too slowly (Greenside et al., 1982). Therefore another method has been suggested to estimate a lower bound for the dimension (Grassberger and Procaccia, 1983) which is discussed in the following.

Instead of counting volume elements or boxes one may count pairs of points $\mathbf{x}(t_i)$, $\mathbf{x}(t_j)$ on a geometrical object which are a distance r_{ij} apart:

$$r_{ij} = |\mathbf{x}(t_i) - \mathbf{x}(t_j)|. \tag{2.9}$$

The number $N(l)$ of such pairs, whose distance is smaller than the prescribed threshold, $r_{ij} < l$, is formally determined by

$$N(l) = \sum_{i,j=1}^{N} \theta(l - r_{ij}), \tag{2.10}$$

where θ is the Heaviside-function with $\theta(a) = 0$ or 1, if $a > 0$ or <0; N is the total number of points. This leads to a cumulative distribution function, which is normalized by the total of N^2 pairs:

$$(1/N^2)N(l).$$

It describes how the number of pairs grows with increasing distance threshold l. For $N \to \infty$, the growth rate changing with the dimension d is determined by the cumulative distribution function

$$C(l) = \lim_{N\to\infty} N(l)/N^2 \sim l^d. \tag{2.11}$$

For example, consider data points homogeneously distributed on a line (on a surface or in a volume); then the number of all points that are up to a distance l apart grows linearly (quadratic or cubic) with increasing l; i.e. proportional to l (l^2 or l^3).

Now the dimension of a geometrical object, say an attractor in phase space, can be determined by the cumulative frequency distribution $C(l)$ of distances of pairs of points which are situated on the time trajectory of the dynamical system; the slope of the distribution, i.e., $\ln C(l)$ versus $\ln l/l_0$, leads to the dimension

$$d = \ln C(l)/(\ln l/l_0). \tag{2.12}$$

The exponent (or correlation exponent) defined by (2.11) is closely related to the exponent (or capacity) given by (2.7), but never greater. In most cases analyzed (Grassberger and Procaccia, 1983a) this inequality is rather tight. Furthermore, one should notice that these definitions of dimension are asymptotic measures.

c. *Scaling: Dimension of attractors*

The dimension of attractors of a dynamical system (after decay of the transients) can be estimated if the results of the foregoing two subsections are combined. This leads to the following procedure:

First, one starts from the time series $x(t)$ as it evolves in the $m = 1$ dimensional phase space, and estimates the related dimension $d(m = 1)$ of the time evolution from the distribution function $C(l) \sim l^d$ (2.11):

$$C_1(l) \sim l^{d\,(m=1)} \quad \text{from } x(t).$$

This is represented by points distributed on a line (i.e., in a one-dimensional phase space $m = 1$). Next the dimensionality $d(m)$ of the phase portrait or time evolution is deduced from the distribution $C(l)$ in successively higher dimensional phase spaces; i.e., proceeding from a two-dimensional display

$$C_2(m) \sim l^{d\,(m=2)}$$

from $x(t)$, $x(t)$ or $x'(t)$, $x(t + \tau)$ to the m-dimensional phase space

$$C_m(l) \sim l^{d(m)} \quad \text{from}$$
$$x(t), x'(t), \ldots, x^{(m-1)}, \quad \text{or}$$
$$x(t), x(t + \tau), \ldots, x[t + (m - 1)\tau] \tag{2.13}$$

until the introduction of a further phase space coordinate $x(t + m\tau)$ or $x^{(m)}(t)$ stops to increase the dimension $d(m)$ of the attractor, on which the dynamics evolves: $d_\infty = d(m) = d(m + 1) = \cdots$, i.e. the estimates of the Grassberger and Procaccia (1983a) algorithm are asymptotic. Thus specifying the (low) dimensionality of an attractor, d_∞, depends on the condition that the sequence of d's departs rapidly from $d = m$ to distinguish the dynamics from random signals. (See random trajectories, this section.) Now the d_∞-dimensional attractor of the original dynamical system (whose independent variables or dimension need not necessarily be known) is embedded in the m-dimensional phase space of derivatives (or time shifted coordinates) of the single state variable. The limiting or saturation value d_∞ defines the dimension of the attractor, on which the dynamics evolves. A noninteger value d_∞ indicates chaotic behavior; the underlying dynamics is deterministic and shows a sensitive dependence on the initial conditions.

The nearest integer above the saturation slope provides the minimum number of independent variables necessary to model the dynamics on the attractor; a reasonable upper bound for the number of variables sufficient to model the dynamics of the attractor is the number of embedding dimension m whose saturation is achieved at $d_\infty(m)$. Thus the distinction between the number of variables necessary to model the dynamics and the number of variables sufficient to do so should be made: 1) Certainly it is impossible to model the dynamics of an attractor with fewer variables than its dimension. Thus one needs at least as many variables as the next integer above its fractal dimension. 2) It holds the analogy with a $d_\infty = 2$ dimensional surface

which cannot generally be embedded in an $m = 2$ dimensional Euclidean space—usually $m = 3$ (or even 4) dimensions—are required. For a dynamical system (together with its attractor) the theorem of Takens (1981) provides the embedding and the Grassberger-Procaccia (1983) algorithm succeeds at the embedding dimension m, where saturation is achieved. Thus, this embedding dimension m resulting from empirical runs, is a good upper bound for the number of variables sufficient to model the dynamics of the attractor.

One may notice that with increasing embedding dimension m the limiting value d_∞ might be slowly approached and not abruptly leaving the diagonal $d(m) = m$ at d_∞. This would be due to the fact that the transformation to the single state variable (and its derivatives or time shifts) does not necessarily represent the minimum state variables, which describe the attractor sufficiently; these may be others. Two further aspects need to be discussed: random trajectories and noisy attractors.

1) Random trajectories

Consider a random time series or points which are homogeneously distributed in phase space. They reveal a dimensionality $d(m)$ which grows with each new dimension or coordinate added to the phase space $x(t)$, $x'(t)$, ... or $x(t)$, $x(t + \tau)$, ..., because random data are independent. Therefore, the dimension of (such a random) time series reveals an "attractor" whose d dimension grows proportional to the number m of the embedding coordinates: $m = d(m)$ or $m + i = d(m + i)$. A random data set of finite length (number of observations) and produced by a random number generator is not expected to follow the proportionality, $d = m$, but merely the inequality, $d \leq m$. Thus in a $(d - m)$-diagram the "random attractor" dimension $d(m)$ would stay close to the diagonal only if the time series is sufficiently long to fill the m-dimensional embedding space. Shorter random time series would enhance the inequality $d \leq m$ (i.e., deviate from the diagonal $d = m$) at smaller embedding dimensions m (see e.g., Fig. 4a, b, c) but without reaching a saturation value d_∞ for increasing m.

However, nonrandom time series with deterministic dynamics represent structures and reach a limiting dimension d_∞. This dimension may be noninteger (i.e., fractal) which is characteristic for irregular or chaotic deterministic processes.

2) Noisy attractors

For experimental situations or observations in nature, it is unavoidable that noise destroys parts of an attractor, in particular, if it is fractal. Embedding the attractor in an m-dimensional space, the noisy trajectory will be space filling (i.e., $d \approx m$) on a length scale smaller (but not larger) than the noise strength; i.e., not unlike a random time series; the distribution function yields

$$C_m(l) \sim l^m \quad \text{for} \quad l < l_{\text{noise}}$$

with increasing embedding dimension m. Whereas for length scales larger than the noise level, the distribution function scales

$$C_m(l) \sim l^d \quad \text{for} \quad l > l_{\text{noise}}$$

with increasing embedding dimension m. The appropriate algorithm proposed by Ben-Mizrachi et al. (1984) can be described as follows: One reconstructs embedding spaces of increasing dimension m with plots $\ln C(l)$ versus $\ln l/l_0$. Above the length scales characterizing the noise the curves should be linear with a slope equal to d; all curves should break at the same length scale l below which a slope proportional to m (embedding dimension) should appear. The position of the break $l = l_{\text{noise}}$ supplies information on the noise level of the system. Furthermore, the dimension of the deterministic part of the noisy attractor can be evaluated for scales beyond noise level.

3. Application to weather and climate variables

The method of estimating the dimension of attractors is applied to time series of various variables representing the weather and the climate system. The results should be considered with the following background information: 1) The time series must be sufficiently long to guarantee convergence of the cumulative distribution function $C(l)$, in particular if the dimensionality of the attractors is large; 2) the selected weather or climate variables need not necessarily be the best representative of the dynamical system, because noise (or other scales) may affect one variable more than the other.

Daily values of surface pressure and relative sunshine duration are selected as time series representing the local weather at a single station (Berlin–Dahlem). The 500 mb geopotential amplitude of zonal wavenumber 5 along 50°N supplements the analysis with a large-scale variable of the weather dynamics. A random time series is attached to each weather and climate variable. It is calibrated by the observed time series to have the same length N, mean and variance but representing Gaussian noise (produced by a random number generator). These random time series are subjected to the same embedding procedure as the observed variable. However, time shifts τ are not changed but fixed at the sampling time $\tau = \Delta t$ (see also section 2c, random trajectories). The method of analysis follows the same procedure for all variables, which is shown in some detail for the daily surface pressure; the other variables are treated analogously.

a. Surface pressure

Daily surface pressure records (0600 GMT at Berlin) are analyzed: 1) a complete 15-year period ($N = 5475$ data points) up to an embedding dimension $m = 20$; 2) seasonal data sets of 14 winter and 15 summer seasons; each season lasts 120 days commencing on 1 November and 1 May, respectively; 3) random processes related to the data sets.

1) EMBEDDING

To visualize the embedding procedure the single station pressure time series $p(t)$ is graphically displayed using values of a randomly chosen winter season (Wi 1978/79). The phase space is spanned by $m = 3$ coordinates (Fig. 1). The horizontal axis describes the time series $x(t) = p(t)$; the vertical axis represents the time series shifted by τ, $x(t + \tau) = p(t + \tau)$ and the axis sloping into the plotting plane denotes twice the time shifts $x(t + 2\tau) = p(t + 2\tau)$. Here it should be noted that only for this display a pressure sampling time of 3 hours (and not of 1 day) is used. For time shifts $\tau = 3$ hours the pressure time evolution in the three-dimensional phase space $p(t)$, $p(t + \tau)$, $p(t + 2\tau)$ stays closely along the main diagonal indicating persistence from $p(t)$ to $p(t + 3h)$ and to $p(t + 6h)$ (Fig. 1a). For $\tau = 1$ day the persistence still prevails but the domain where the trajectory evolves broadens (Fig. 1b). For time shifts corresponding to the decorrelation time $\tau = 3$ days (macro- or integral-time scale) the trajectory becomes space filling (Fig. 1c). This is valid also for time shifts $\tau > 3$ days; it guarantees data independence. For $\tau \gg 3$ days the always existing noise in weather systems dominates the deterministic dynamics. Therefore, for practical purposes the most appropriate τ needs to be selected by comparing results of increasingly larger time scales.

2) DIMENSION (CUMULATIVE FREQUENCY DISTRIBUTION)

The cumulative frequency distribution functions $C(l)$ of distances of daily pressure values evolving in the m-dimensional embedding spaces are shown for the basic time scale $\tau = 3$ days, which corresponds to the decorrelation time of synoptic disturbances. Analyses of other time shifts are not shown but used for scaling the attractor dimension. The distribution functions (2.11) are presented in log-coordinates to determine the slope (2.12). The cumulative number of pressure distances $r_{ij} < l$ grows with increasing threshold distance l. When l reaches its upper limit, the distribution functions converge to unity, which holds for all distance distributions. The related embedding dimensions m are obtained from the $C(l)$-graphs in Figs. 2 and 3 (and others). They correspond to the maximum time shifts (or multiple of the time scale τ), by which the independent single variable phase space coordinates are defined. Cumulative distribution functions are evaluated for increasingly higher dimensional phase spaces (i.e., for increasing m) to obtain a sufficient embedding of the attractor in the new phase space of time shifted coordinates. Distribution functions are derived for the complete 15-year record, seasonal data sets of daily pressure values, and the related random series. With increasing embedding dimension m one notices an increasing slope of the distribution functions for all random series as shown in Fig. 4. The same can be observed for the complete 15-year record but not for the summer or winter data sets. The related dimension of the weather attractor can now be deduced by scaling of the distribution functions.

3) SCALING

The scaling of the distribution function $C(l) \sim l^d$ (i.e., the dimensionality of the attractor) is defined by

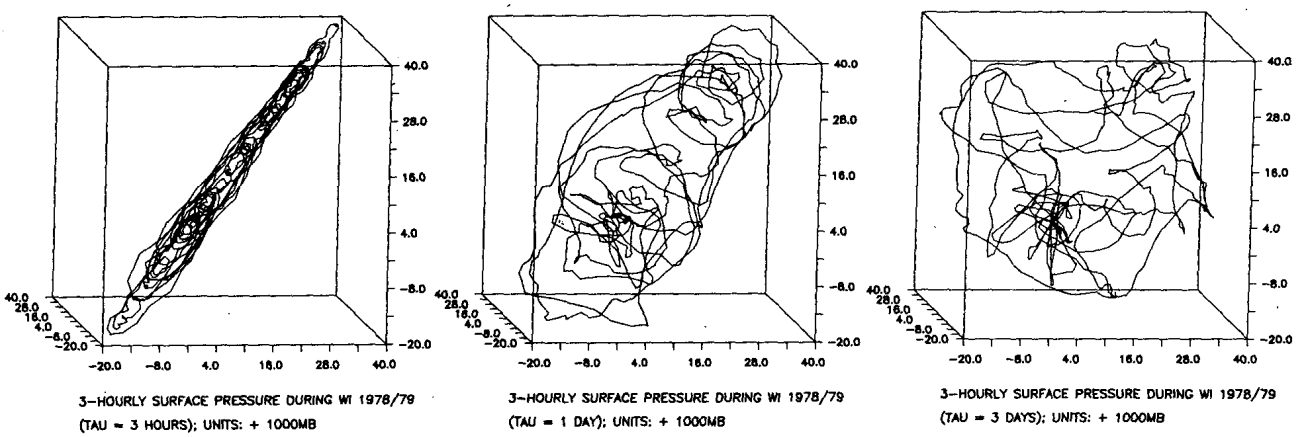

FIG. 1. Time trajectory of three-hourly surface pressure evolving in a three-dimensional phase space of time-lagged pressure coordinates (units: 1000 mb). Horizontal axis: $p(t)$; vertical axis: $p(t + \tau)$; axis into plotting plane: $p(t + 2\tau)$. From left to right: (a) $\tau = 3$ hours, (b) $\tau = 1$ day, (c) $\tau = 3$ days.

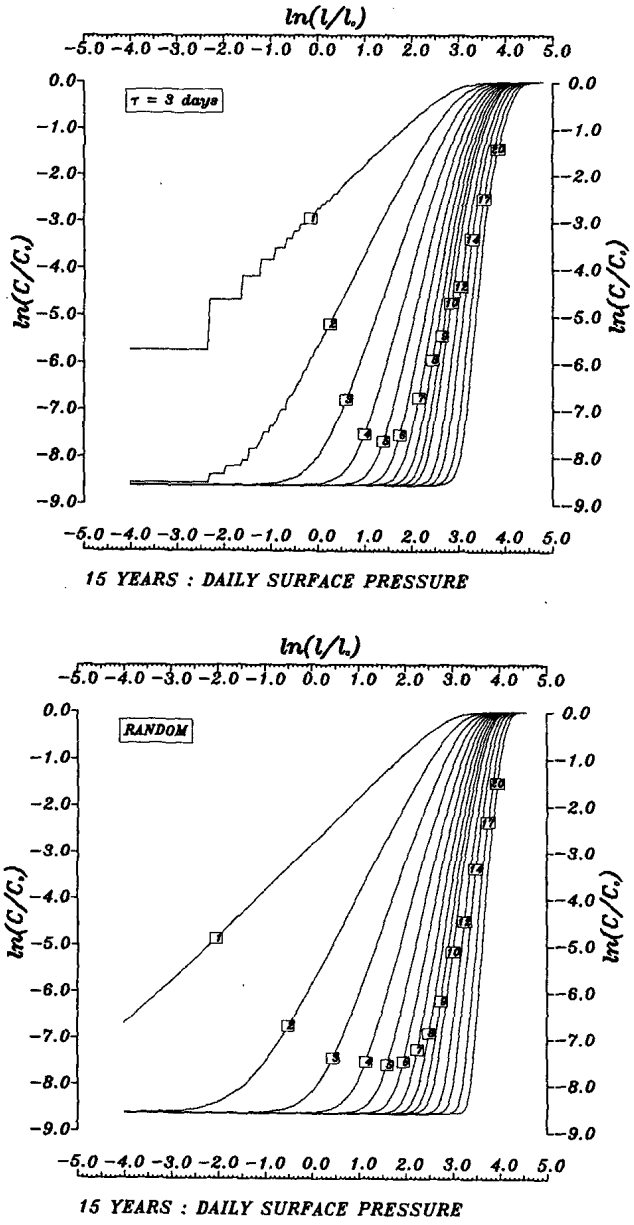

FIG. 2. Cumulative distribution function of distances of the 15-year daily pressure trajectory evolving in m-dimensional phase spaces (m = 1 to 20) of time lagged (τ = 3 days) coordinates of the same variable. Top: observed time series; bottom: related random series of same length, mean and variance.

its slope d in the log$C$ versus log$l$ diagram (Figs. 2 and 3). With increasing embedding dimension m the slopes $d(m)$ of the related $C_m(l)$ tend toward a limiting or saturation value, d_∞, unless the underlying dynamics is a random process. This saturation value defines the dimension of the attractor and a lower limit for the number of independent variables to simulate the dynamics on it. The dimensions $d(m)$ up to a possible saturation dimension d_∞ are deduced for various data sets of the same variable using different time scales τ, which are embedded in m-dimensional phase spaces. The results are compared with the random time series. How the tendency towards saturation proceeds with increasing embedding is shown in a (d, m)-graph presented in Fig. 4a–c. Some results should be noted.

4) RESULTS AND INTERPRETATION

• The dimension of the attractor of the random time series increases with each further coordinate added to the phase space, i.e., with increasing embedding dimension m. For large m, however, the scaling follows

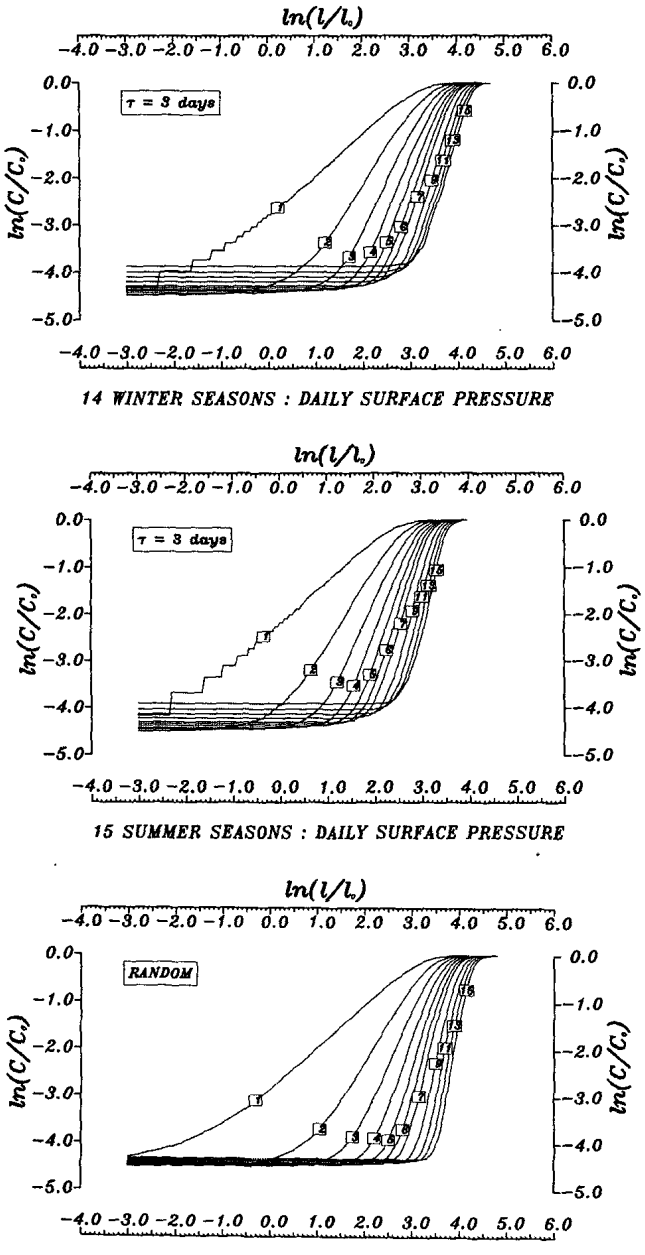

FIG. 3. Cumulative distribution function of distances of seasonal daily pressure trajectories. From top to bottom: (a) 14 winter seasons, (b) 15 summer seasons, (c) 15 randomized seasonal time series.

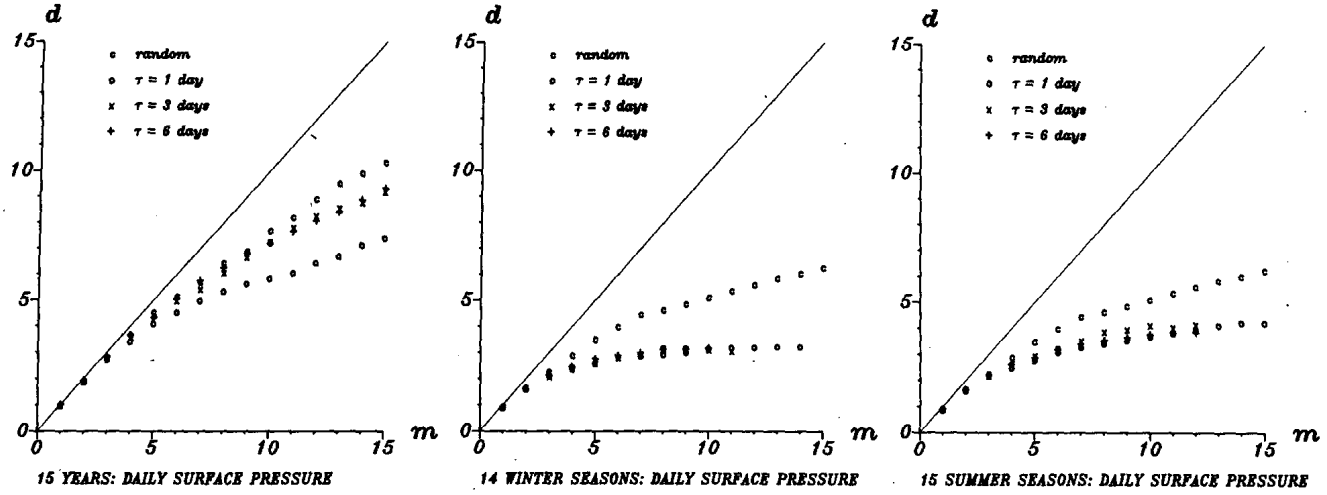

FIG. 4. Dimensionality (d) of the weather attractor as a function of the number m of phase space coordinates, which are determined by multiples (m) the time shifted pressure record (using lags τ = 1, 3 and 6 days). Randomized time series (index c) are compared with observations. From left to right: (a) 15 year record, (b) winter seasons, (c) summer seasons.

$m \geq d(m)$ and not the diagonal, $m = d(m)$, as required. This may be due to the random number generator and/or to the finiteness of the random time series (see section 2c, random trajectories). This empirical random scaling is appended to all dimensionality analyses (signature c) to compare it with the attractor dimensions $d(m)$ derived from the observed data sets (Fig. 4a–c).

• The scaling of the 15-year time series of daily surface pressure increases with increasing embedding dimension. Even at embedding dimension m = 15 to 20, there is no indication that the attractor is sufficiently embedded and has reached its limiting dimension (Fig. 4a). This is not surprising, because the time series includes weather phenomena in winter and summer, the long-range processes from season to season and the interannual variability. A dynamical system, which includes all these aspects, depends on a large number of independent variables (degrees of freedom) and the inherent noise.

• For analyzing weather processes one should not consider the highly nonlinear longtime memory between seasons and years. Instead, the pressure record should be reduced to seasonal samples of 14 winters and 15 summers; each season lasts 120 days commencing on 1 November and 1 May, respectively. Thus, distribution functions are individually evaluated for each season and then composited to discard the long-range processes and interannual variability.

Scaling the weather attractor described by the trajectories of the seasonal time series leads to different results: Increasing the embedding space from dimension m = 1 to 15 and larger, the log-slope d of the distribution function $C(l) \sim l^d$ increases until a saturation value d_∞ is attained. This value may now be interpreted as the dimension of the local weather attractor. There are different values for summer and winter with larger attractor dimension in summer. For correlation times $\tau \geq 3$ days, linear independence of the data sets is satisfied and one observes an attractor dimension $d_\infty \approx 3.2$ for winter seasons ($d_\infty \approx 3.9$ for summer seasons). The observed fractal dimensionality indicates the deterministic chaos of the weather system with its supposed sensitivity on initial conditions. The result of this analysis that summers and winters separately provide small dimensions but the annual data do not, seems to be valid if there are two distinct regimes of flow for the two seasons rather than just one regime for which a value of a parameter (e.g., the latitudinal temperature gradient) is changing between seasons.

Finally, a physical interpretation may be suggested for the observed low-dimensionality of the weather attractor: Weather fluctuations are realized as cyclones (short period disturbances), ensembles of which (cyclone families) are attached to the troughs of slowly traveling major waves. These two distinct types of synoptic disturbances arrange themselves in an index cycle of enhanced and reduced synoptic activity. These three processes are realized by three distinct but broad spectral peaks in local time series (Fraedrich et al., 1979), hemispheric wavenumber-frequency analyses (Fraedrich and Böttger, 1978) and, of course, phenomenological observations. It is suggested that the number of three weather phenomena of independent periodicity coincides with the integer part of the estimated fractal dimensionality; i.e., the integer part of the saturation dimension d_∞ seems to define the number of fundamental periods in the process. (See, also, section 3d on the climate variable.)

• The next integer above the fractal saturation dimension ($d_\infty < 4$) provides the minimum number of independent variables necessary to model the dynam-

ics. The saturation is achieved at $m < 10$ which is a good (estimate of the) upper bound for the number of variables sufficient to model the dynamics of the attractor. These results should not suggest that the weather (in Germany) may be modeled on the pressure reading of one station (Berlin), but that one projection of the attractor (obtained by applying the Grassberger–Procaccia (1983) algorithm to this record) happens to reveal a small dimension. Similar contributions from projections obtained by evaluating records at other distant stations are expected, which then would add up to the true dimension of the attractor.

b. Sunshine duration

Daily sunshine hours (from Campbell–Stokes sunshine recorders) are normalized by the astronomically possible sunshine duration and using an estimated correction for the horizontal extinction of 1.5 degrees for both sunrise and sunset. This leads to a new time series of the relative sunshine duration per day, $\theta \leqslant \theta(t) \leqslant 1$ which is analyzed in this subsection. Its complement $1 - \theta$ is an approximation to the daytime average of areal cloud cover. The 30-year period is evaluated as a whole and separated for 29 winter and 30 summer seasons. The embedding procedure of the single station sunshine time series $\theta(t)$ is graphically displayed (Fig. 5) using observed values of the randomly chosen year 1958. Again, the phase space is spanned by three coordinates: the horizontal axis describes the time series $x(t) = \theta(t)$; the vertical axis represents the time series shifted by τ: $x(t + \tau) = \theta(t + \tau)$; and the axis sloping into the plotting plane denotes twice the time shift, $x(t + 2\tau) = \theta(t + 2\tau)$. For $\tau = 1$ day (corresponding to the sampling time) the time evolution of sunshine duration is space filling. The cumulative distribution functions $C(l)$ of sunshine distances in the m-dimensional (embedding) space are not shown, but the results of scaling ($C(l) \sim l^d$) the attractor dimension (Fig. 6). They are comparable with the pressure record:

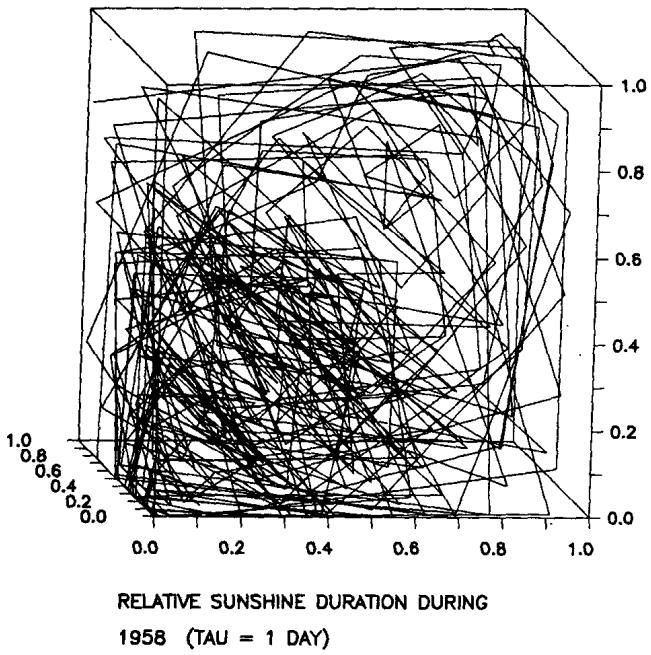

FIG. 5. Time trajectory of daily relative sunshine duration θ evolving in a three-dimensional phase space of time lagged sunshine series. Horizontal axis: $\theta(t)$; vertical axis: $\theta(t + 1$ day); axis into plotting plane: $\theta(t + 2$ days).

- The dimension of the randomized time series increases with increasing embedding dimension m; for large m, however, the scaling follows $m \geqslant d(m)$ and not the diagonal, $d(m) = m$, as required.
- The scaling of the attractor of the complete time series of 30 consecutive sunshine-years shows similarity with its related randomized data set; with increasing τ (i.e., growing data independence) this similarity rises (Fig. 6a).
- Scaling the weather attractor by seasonal time series leads to different results (Fig. 6b, c). Increasing the embedding space from dimension $m = 1$ to 15 and larger, the log-slope d of the distribution function $C(l) \sim l^d$ increases until a saturation value d_∞ is attained. Again this value may now be interpreted as the dimension of the local weather attractor. There are different values for summer and winter with larger attractor dimensions in summer. For correlation times $\tau \approx 3$ days, linear independence of the data sets is satisfied. However, one may notice the unusually bad—yet unexplained—properties $d(m)$ for $\tau = 3$ days in winter (Fig. 6b). One observes an attractor dimension $d_\infty \approx 3.1$ for winter seasons ($d_\infty \approx 4.3$ for summer seasons). The observed fractal dimensionality indicates the deterministic chaos of the weather system with its supposed sensitivity on initial conditions. The next larger integer above saturation dimension ($n \geqslant d$) provides the minimum number of variables necessary to model the behavior of the dynamical system on the attractor with four key variables in winter and five in summer; an estimate of the upper bound for the number of variables sufficient to model the dynamics would be $m \leqslant 10$. Still, the caveat added to the results and interpretation of the surface pressure analysis (section 3a) applies also to the local sunshine duration.

The results of the sunshine analysis lead to some additions to interpretation of the pressure record: Each weather variable has a different sensitivity on influences of other scales and noise. This is reflected by the summer sunshine duration with convection playing a non-negligible role, which seems to be reduced in the daily pressure record with less dimensionality in summer. But, the low dimensionality of the weather attractor is supported by both daily pressure and sunshine duration. Furthermore, its fractal values reflect the deter-

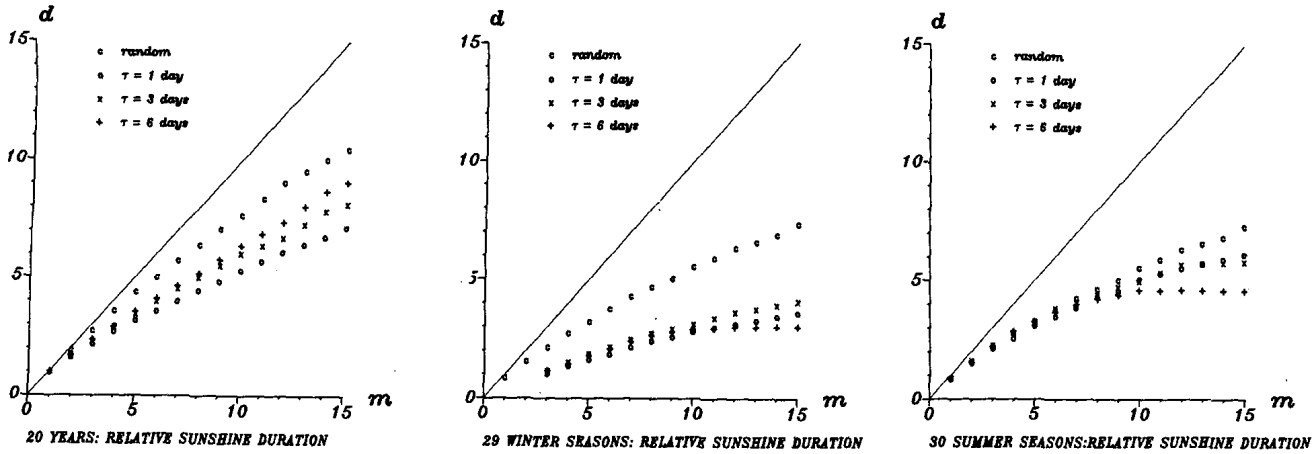

FIG. 6. As in Fig. 4 but for daily relative sunshine duration. From left to right: (a) 30-year record, (b) 29 winter seasons, (c) 30 summer seasons.

ministic chaos (or strong dependence on initial conditions) characterizing the weather dynamics.

c. *Zonal wave amplitude*

Daily amplitudes of the 500-mb geopotential waves along 50°N define large-scale hemispheric weather variables. The results of dimensionality analyses are shown for wavenumber 5 (Fig. 7) which are based on a ten-year period; similar conclusions are also deduced from the amplitudes of other waves. They support the general results drawn from the local weather time series: The complete time series, including interannual variability, does not provide a low saturation dimension (Fig. 7a). But the seasonal data sets support the low dimensionality of the weather attractor (with $d_\infty \approx 3$ in winter and $d_\infty \approx 3.6$ in summer). Again, the nonlinear interaction of three independent synoptic or weather scales is suggested for the low dimensionality of the weather attractor. Spectra in the wavenumber-frequency domain reveal three peaks of the zonal transient eddy variance. They refer to progressive long and short waves, which are realized by cyclones and cyclone families (see section 3a), and quasi-stationary ultralong waves, which consist of barotropic westward and baroclinic eastward components (related to the index cycle of enhanced and reduced activity). Furthermore, intensity maxima of both local and zonal spectra vary considerably from season to season (e.g., Hartmann, 1974; Fraedrich and Böttger, 1978). This may account for the required fourth independent variable, but keeping the weather attractor dimension fractal between three and four with its associated deterministic chaos.

d. *A climate variable: Oxygen isotope record*

The analysis of a climate attractor is based on a detailed oxygen isotope record of planktonic species (Sarnthein et al., 1984). It is gained from a 10.7 m long

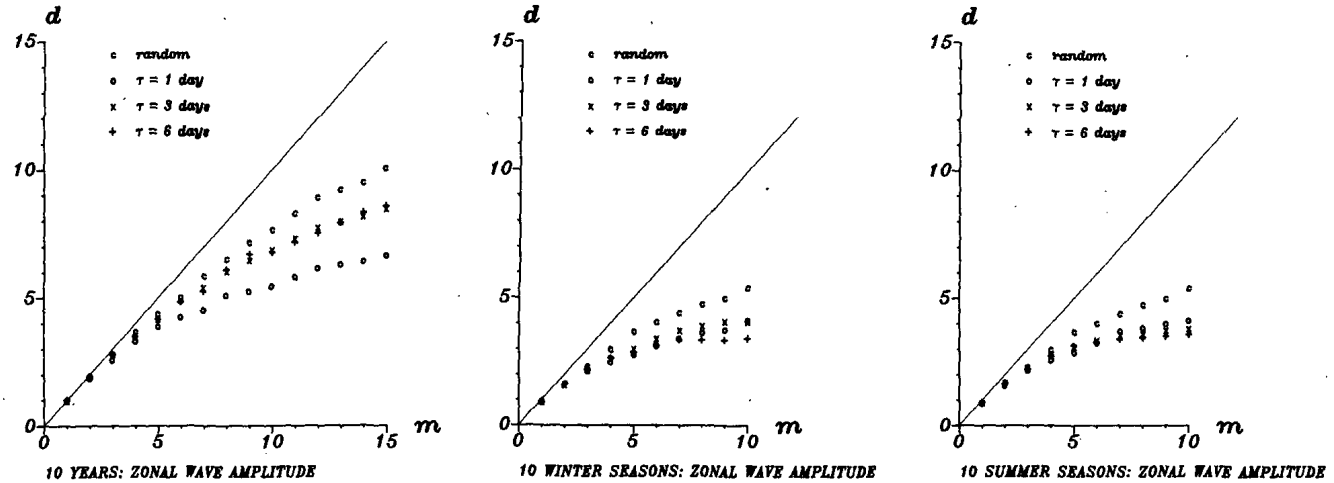

FIG. 7. Same as Fig. 4 but for daily amplitudes of 500-mb zonal wavenumber 5. (a) 10 years, (b) 10 winter seasons, (c) 10 summer seasons.

gravity core (Meteor 13519) in the eastern equatorial Atlantic near 5°N and 20°W. There are 182 $\delta^{18}O$ values available which cover an age of 775 000 years bp. They refer to sampling slices of 3 to 7 cm depth corresponding to 2000–4000 years of sedimentation.

Embedding the time evolution ($\delta^{18}O$-series) into a three-dimensional phase space of time (depth) shifted coordinates, one observes a notable space filling of the trajectory which is associated with a certain degree of persistence (along the diagonal; Fig. 8a). Furthermore, there is a limiting dimensionality, if the distance distribution function, $C(l)$ of the $\delta^{18}O$-values is compared with the related randomized time series within increasingly higher dimensional embedding spaces (Fig. 8b, c). This is quantified by scaling the distribution function $C(l) \approx l^d$ (Fig. 8d); i.e., the climate attractor tends toward a saturation dimension $d_\infty \approx 4.4$. The fractal dimensionality characterizes the chaotic dynamics of the otherwise deterministic climate system (and its supposed sensitivity on initial conditions). Thus the minimum number of variables necessary to simulate the climate dynamics on the attractor can be reduced to five key variables. This is not in disagreement with other results ($d_\infty = 3.1$, Nicolis and Nicolis, 1984), which reveal a smaller but also fractal saturation dimension of the climate attractor.

Some comments on the interpretation of the results seem to be in order: First, the climate series of deep sea cores consists only of a limited amount of data from which the statistics is determined. But the conclusion of a low dimensionality of the climate attractor seems to be justified, because the scaling analysis of the related randomized series shows no saturation and its distribution deviates significantly from the observed one (Kolmogoroff–Smirnov test with 99% significance for all embedding dimensions m). Second, not unlike the weather time series (section 3a, b, c) one observes three to five spectral variance density peaks in deep sea cores, which are commonly related to the influence of the earth's orbital parameters (e.g., Kukla et al., 1981; Herterich and Sarnthein, 1984) with the obliquity (41 000 yr; henceforth 41 kyr), precession cycles (19 and 23 kyr), and the eccentricity (410 and 100 kyr). Thus the dimension of the climate attractor can be related to the deterministic dynamics of at least three to five key variables described by a fractal attractor or to the nonlinear response of a system modulated by independent frequencies.

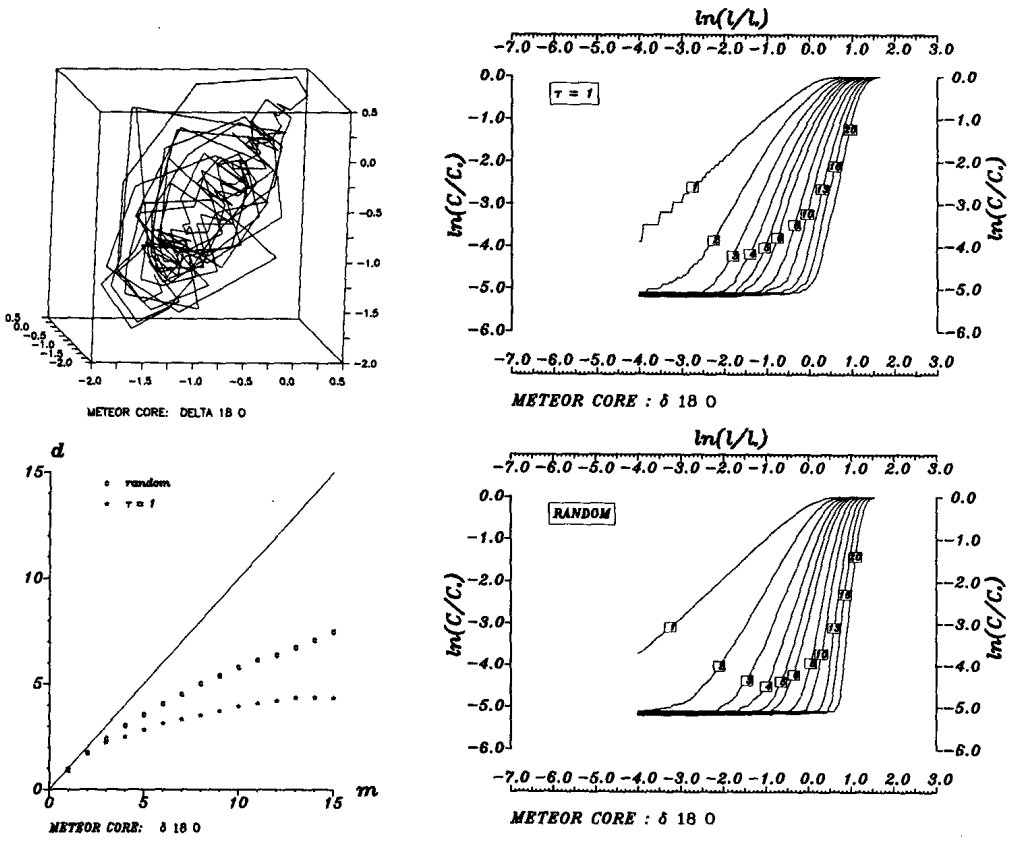

FIG. 8. The climate attractor deduced from Meteor core 13519 (clockwise from upper left): (a) time trajectory of $\delta^{18}O$-values (see Fig. 1), (b) cumulative distance distribution depending on embedding dimension m for observed and (c) randomized records (see Fig. 2), (d) dimensionality d of the climate attractor as a function of the number m of phase space coordinates (see Fig. 4).

4. An independent estimate of the climate attractor dimensionality by empirical orthogonal functions

An independent estimate of dimensionality is applied to the time series of climate data (section 3d). The trajectory (evolving in the phase space of m independent time lagged coordinates of the same variable) is transformed into a phase space of m eigenvectors (empirical orthogonal functions or EOF's). The related time dependent amplitudes or coefficients define the new trajectory.

a. Empirical orthogonal functions

Empirical orthogonal functions are eigenvectors of the symmetric (mxm)-covariance matrix

$$c_{ij} = \langle x[t + (i)\tau]x[t + (j)\tau]\rangle, \quad i, j = 0, \cdots, m - 1 \tag{4.1}$$

whose elements c_{ij} are auto-covariances of the single state variable time series $x(t)$ and its (i or j) shifts by fixed time lags τ (2.4c). Here the variable $x(t)$ has been reduced by its mean; the ensemble averaging $\langle\ \rangle$, is taken over the length of the time series. The resulting m eigenvectors Z_k are m-tuples

$$Z_k = [Z_{k0}, Z_{k1}, \cdots, Z_{k(m-1)}] \quad \text{with} \quad k = 0, \cdots, m - 1 \tag{4.2}$$

each of which consists of m components Z_{kl} with $l = 0, \cdots, m - 1$. The eigenvectors span an m-dimensional space of independent orthogonal coordinates for the time trajectories; they replace the m-dimensional phase space of the time shifted coordinates (2.4c) embedding the attractor. The related time dependent amplitudes

$$a_0(t), \ldots, a_{m-1}(t)$$

are multipliers of the eigenvectors $Z_k = [Z_{k0}, \cdots, Z_{k(m-1)}]$ such that the original time series, its first time shift, etc., can be generated again

$$x(t) = \sum_{l=0}^{m-1} a_l(t)Z_{0,l}; \quad x(t - \tau) = \sum_{l=0}^{m-1} a_l(t)Z_{1,l}; \text{ etc.}$$

Now, it is not the transformation process of the time evolution into the eigenvector space (4.2) (spanned by $Z_0, \ldots, Z_{m-1}$ instead of time shifted coordinates $x(t)$, $\ldots, x[t + (m - 1)\tau]$), which is of relevance for estimating the dimension d of attractors, but the limited number of eigenvectors (or orthogonal coordinates) $d < m$ necessary to describe the time evolution of the system $x(t)$ (2.4c) with sufficient accuracy. This can be achieved by comparing the variances (or eigenvalue λ) which each eigenvector contributes to the total variance integrated over the phase space (i.e., sum of all eigenvalues):

$$\lambda_0 > \lambda_1 > \cdots > \lambda_{m-1}.$$

Although EOFs are of statistical nature they are the optimum set of basis functions for a given truncation ($d < m$), i.e., no other basis set can explain more of the variance averaged over the m-dimensional phase space. The eigenvalues define the variance which the eigenvectors contribute to the time evolution. Their distribution and the related confidence limits lead to a rule of thumb (North et al., 1982; Hsiung and Newell, 1983), to select a relevant subset of d ($<m$) eigenvectors which describes the dynamics of the time series with sufficient accuracy. This subset consists of d consecutive eigenvectors which provide another estimate of the attractor dimension. The remaining variance contribution is taken as noise and may be interpreted as adding to the fractal dimensionality of the attractor.

The climate record (Meteor core $\delta^{18}O$) evolving in an m-15 dimensional phase space of shifted coordinates leads to the same number of EOF's. The related eigenvalues (and their variance contributions) are presented in Fig. 9. The relevant subset of consecutive eigenvectors, which lead to dimension of the climate attractor, is evaluated in the following.

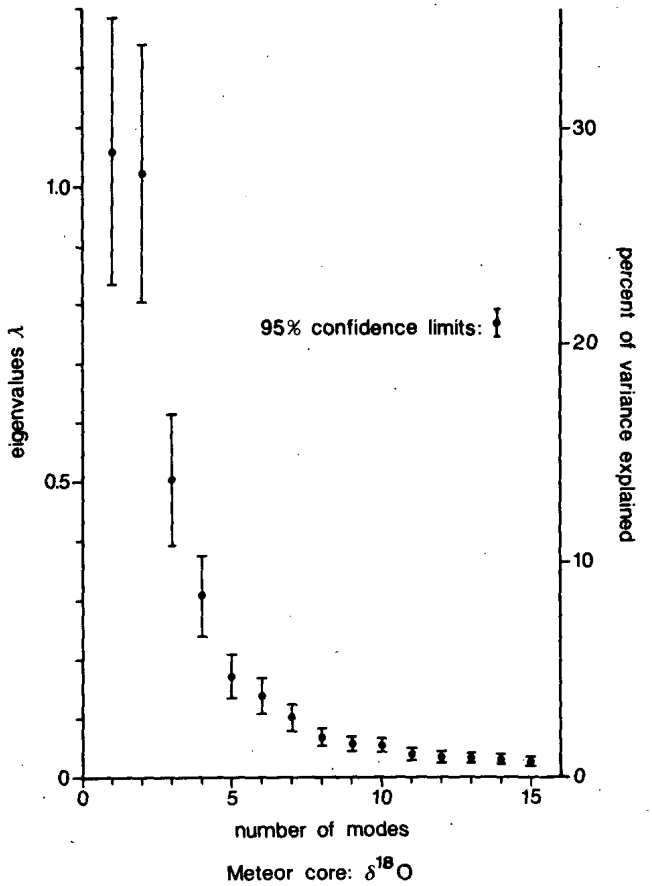

FIG. 9. The eigenvalues and the associated 95% confidence interval for $m = 15$ modes. They are related to the embedding phase space spanned by $m = 15$ coordinates of the time lagged variable $\delta^{18}O$ of the Meteor core. The right axis denotes the percentage of phase space variance explained by each eigenvector.

b. Confidence limits

A 95% confidence interval $\delta\lambda$ can be placed to each eigenvalue

$$\delta\lambda \sim 2\lambda\sqrt{2/N} \tag{4.3}$$

with sample size N. It describes the intersample variability of each EOF. Thus, if the confidence interval $\delta\lambda$ of a particular eigenvalue λ is comparable or larger than the spacing between λ and one of its neighbors, then the confidence interval $\delta\lambda$ of the EOF associated with λ is comparable with the (size of) neighboring EOF. Thus groups of two or more EOFs can be defined whose eigenvectors are indistinguishable from one another in terms of their confidence intervals and contributions to the total variance; this is based on the following: if a set of two or more EOFs has the same eigenvalue, any linear combination of the members is also an EOF with the same eigenvalue. This ambiguity in choosing the proper eigenvector or a linear combination may characterize noise effects if the largest modes with smallest variance contributions are considered. This holds for the modes 5 to 15 (in Fig. 9).

For smaller mode numbers (and larger variance contributions) the ambiguity indicates that (as it appears in Fig. 9) the first pair of EOFs derived from the record, is likely to be mixed by sampling errors.

However, the first four eigenfunctions all have confidence intervals smaller than the spacing to the following modes; i.e., the subset or group of the first four eigenvectors defines the signal of the time series, which is separated from the noise represented by the remaining eigenvectors. Thus the dimensionality estimate of the climate attractor (as deduced from the eigenvector analysis) leads to four independent variables; the intrinsic noise effects demand at least one further variable to obtain the fractal value of the saturation dimension $d_\infty \sim 4.4$ (deduced in section 3d).

5. Conclusions and outlook

Based on single variable time series the dimensions of weather and climate attractors are evaluated to obtain a lower bound on the number of essential variables needed to model the dynamics. Furthermore, an upper bound for the number of variables sufficient to model the dynamics of the attractor can also be estimated. The procedure is based on the cumulative distribution of the distances of all data points (time trajectories) as they occur in phase spaces. They are spanned by an increasing number of independent coordinates to obtain a sufficient embedding of the attractor of the dynamical system; the coordinates are defined by the single variable time series and its time lags. Various weather variables (local pressure, relative sunshine duration and zonal wave amplitudes) are analyzed and compared with random data sets. For all variables one observes a low dimensionality (between three and four) of the weather attractor, if interannual variability and seasonal variations are excluded by using seasonal data sets. The observed fractal dimensionality accounts for a chaotic dynamical system and its strong dependence on initial conditions. A qualitative physical interpretation of the deduced low and fractal dimensionality is suggested.

A climate variable (the δ^{18}O-record of the Meteor core 13519 in the tropical Atlantic) reveals a dimensionality of 4.4 for the climate attractor, suggesting that a minimum of five independent variables is necessary to model its dynamics. Finally, an independent method to estimate the dimensionality of attractors is suggested and applied to the climate record. It is based on a transformation of the phase space trajectories into a space of empirical orthogonal functions (eigenvectors). A subset of eigenvectors, which may be separated by noisy contributions by prescribed confidence limits, is sufficient to describe the time evolution in phase space. The related number of these relevant eigenvectors supports the dimensionality analysis of the climate record based on the cumulative distance distribution functions.

These methods may serve as a further test of the performance of the dynamics of weather and climate models to support the phenomenological and physical or standard circulation statistics used so far. The new aspect introduced to model verification would be an analysis of its behavior in phase space. Finally, it should be noted that the dimensionality of the attractors of dynamical systems is only the first level of knowledge to describe its properties. The second level may be the evaluation of the independent variables.

Acknowledgments. Parts of the paper were written during a visit at the Max-Planck-Institut für Meteorologie; the fruitful discussions and support of K. Hasselmann and H. Hinzpeter are gratefully acknowledged. The constructive comments of the two referees and discussions at the Jülicher Kreis "Nonlinear Dynamics" are appreciated. Thanks are due to Ms. M. Scholz and S. Parker for typing, and M. Lutz and H. Haug for computing and plotting assistance.

REFERENCES

Ben-Mizrachi, A., I. Procaccia and P. Grassberger, 1984: Characterization of experimental (noisy) strange attractors. *Phys. Rev. A.*, **29**, 975–977.

Böttger, H., and K. Fraedrich, 1980: Disturbances in the wavenumber–frequency domain observed along 50°N. *Contr. Atmos. Phys.*, **53**, 90–105.

Brandstäter, A., J. Swift, H. L. Swinney, A. Wolf, J. D. Farmer, E. Jen and P. J. Crutchfield, 1983: Low-dimensional chaos in a hydrodynamic system. *Phys. Rev. Letters*, **51**, 1442–1445.

Charney, J. G., and F. G. DeVore, 1979: Multiple flow equilibria in the atmosphere and blocking. *J. Atmos. Sci.*, **36**, 1205–1216.

Craddock, J. M., and C. R. Flood, 1969: Eigenvectors for representing the 500 mbar geopotential surface over the Northern Hemisphere. *Quart. Roy. Meteor. Soc.*, **95**, 576–593.

Eckmann, J. P., 1981: Roads to turbulence in dissipative dynamical systems. *Rev. Modern Phys.*, **53**, 643–654.

Farmer, D., E. Ott and J. A. Yoshe, 1983: The dimension of chaotic attractors. *Physica*, **7D**, 153–180.

Fraedrich, K., and H. Böttger, 1978: A wavenumber–frequency analysis of the 500 mb geopotential at 50°N. *J. Atmos. Sci.*, **35**, 745–750.

——, —— and Th. Dümmel, 1979: Evidence of short, long and ultralong period fluctuations and their related transports in Berlin rawinsonde data. *Contrib. Atmos. Phys.*, **52**, 348–361.

Froehling, H., J. P. Crutchfield, D. Farmer, N. H. Packard and R. Shaw, 1981: On determining the dimension of chaotic flows. *Physica*, **3D**, 605–617.

Grassberger, P., and J. Procaccia, 1983a: Measuring the strangeness of strange attractors. *Physica*, **9D**, 189–208.

——, 1983b: Characterization of strange attractors. *Phys. Rev. Letters*, **50**, 346–349.

Greenside, H. S., A. Wolf, J. Swift and T. Pignataro, 1982: Impractability of a box-counting algorithm for calculating the dimensionality of strange attractors. *Phys. Rev. A*, **25**, 3453–3456.

Guckenheimer, J., 1982: Noise in chaotic systems. *Nature*, **298**, 358–361.

——, and G. Buzyna, 1983: Dimension measurements for geostrophic turbulence. *Phys. Rev. Letters*, **51**, 1438–1441.

Hartmann, D., 1974: Time spectral analysis of midlatitude disturbances. *Mon. Wea. Rev.*, **102**, 348–362, Corrigendum 541–542.

Herterich, K., and M. Sarnthein, 1984: Brunhes time scale: Tuning by rates of calcium–carbonate dissolution and cross spectral analyses with solar insolation. *Milankovitch and Climate*. A. Berger, and J. Imbrie, Eds., NATO–ASI–Series C–126.

Hirsch, M. W., 1976: *Differential Topology. Graduate Texts in Mathematics*, Springer–Verlag, 221 pp.

Hsiung, J., and R. E. Newell, 1983: The principal nonseasonal modes of variation of global sea surface temperature. *J. Phys. Ogr.*, **13**, 1957–1967.

Kukla, G., A. Berger, R. Latti and J. Brown, 1981: Orbital signature of interglacials. *Nature*, **290**, 295–300.

Lorenz, E. N., 1963: Deterministic nonperiodic flow. *J. Atmos. Sci.*, **20**, 130–141.

Mandelbrot, B. B., 1977: *Fractals: Form, Chance, and Dimension*. Freeman and Co., 365 pp.

Nicolis, C., and G. Nicolis, 1984: Is there a climatic attractor? *Nature*, **311**, 529–532.

North, G. R., T. L. Bell, R. F. Cahalan and F. J. Moeng, 1982: Sampling errors in the estimation of empirical orthogonal functions. *Mon. Wea. Rev.*, **110**, 75–82.

Packard, N. H., J. P. Crutchfield, J. D. Farmer and R. S. Shaw, 1980: Geometry from a time series. *Phys. Rev. Letters*, **45**, 712–716.

Roux, J.-C., R. H. Simoyi and H. L. Swinney, 1983: Observation of a strange attractor. *Physica*, **8D**, 257–266.

Ruelle, D., 1981: Chemical kinetics and differentiable dynamical systems. *Nonlinear Phenomena in Chemical Dynamics*. A. Pacault, and C. Vidal, Eds. Springer–Verlag, 30–37.

Russell, D. A., J. D. Hanson and E. Ott, 1980: Dimension of strange attractors. *Phys. Rev. Letters*, **45**, 1175–1178.

Sarnthein, M., H. Erlenheuser, R. von Grafenstein and C. Schröder, 1984: Stable–isotope stratigraphy for the last 750,000 years: Meteor core 13519 from the eastern equatorial Atlantic. *Meteor. Forsch. Ergebn.*, C–38, 9–24.

Silberman, I., 1954: Planetary waves in the atmosphere. *J. Meteor.*, **11**, 27–34.

Takens, F., 1981: Detecting strange attractors in turbulence. *Dynamical Systems and Turbulence*. Warwick, Springer–Verlag, 366–381.

Whitney, H., 1936: Differentiable manifolds. *Ann. of Math.*, **37**, 645–680.